

A study of the asymmetry in the H₂O maser line at $\lambda = 1.35$ cm on the base of the hyperfine structure

E. E. Lekht¹, N. A. Silant'ev¹, G. M. Rudnitskij², and G. A. Alexeeva³

¹ Instituto Nacional de Astrofísica, Óptica y Electrónica, Luis Enrique Erro No. 1, Apartado Postal 51 y 216, CP 72840 Tonantzintla, Puebla, México
e-mail: lekht@inaoep.mx

² Sternberg Astronomical Institute, 13 Univetsitetskij prospect, Moscow, 119992, Russia

³ Main (Pulkovo) Astronomical observatory of Russian Academy of Sciences, Pulkovskoe shosse 65, St.-Petersburg, 196140, Russia

Received 21 April 2008 / Accepted 30 September 2008

ABSTRACT

The results of analyzing asymmetry in the H₂O maser lines at $\lambda = 1.35$ cm are presented. We investigated in detail the known mechanism of the asymmetry origin due to the hyperfine structure of the $6_{16} \rightarrow 5_{23}$ transition and different (not equidistant) positions of the corresponding triplet components. The triplet of the lines is characterized by the sum of extinction factors that are continuously transformed into a single-peaked asymmetric extinction coefficient, with the increase in the Doppler widths (characterizing by effective Doppler velocity u_D). A noticeable asymmetry corresponds to $u_D \leq 0.5\text{--}1$ km s⁻¹. For higher values of u_D the extinction factor approaches a Gaussian shape with the decreasing magnitude of the profile asymmetry. An appreciable asymmetry in unsaturated maser lines can only arise at $u_D \leq 0.5$ km s⁻¹, if there are very narrow linewidths ($\Delta u \approx 0.2\text{--}0.4$ km s⁻¹). But observed saturated masers possess a fairly high degree of the line asymmetry, 10–40%. Most probably, this asymmetry is a result of rebroadening of the linewidth up to the value that is comparable to the width of the asymmetric extinction coefficient.

Key words. line: profiles – masers – radiative transfer

1. Introduction

Long-term monitoring of the H₂O maser emission sources at $\lambda = 1.35$ cm in active star-forming regions has shown the existence of separate lines (emission features) with various linewidths and shapes. The linewidths of the emission from such single features can be from 0.35 to 0.9 km s⁻¹. The linewidth is determined by thermal and small-scale turbulent motions of H₂O molecules in a maser spot. The line shape is determined by possible superposition of some components with similar radial velocities. In the case of a single spectral line, which is emitted by a separate feature, the line shape is basically approximated by the usual Gaussian curve. The monitoring has shown that there are single lines with non-Gaussian shapes, and these lines mostly have an asymmetric shape.

Silant'ev et al. (2002) have shown that the line asymmetry can arise in the propagation of radiation in the surrounding medium with non-inverted populations of molecular energy levels if this medium is moving with respect to a maser spot. If the non-inverted layer moves toward the maser spot, the high-frequency side of the maser spectral line is more intense than the low-frequency side, and vice versa. This is not an “intrinsic” mechanism, because the asymmetry arises beyond the maser “spot”.

Another “intrinsic” mechanism was proposed by Varshalovich et al. (2006). It is based on the existence of the hyperfine structure of the energy level corresponding to the transition at $\lambda = 1.35$ cm. In this mechanism the maser line consists of three lines near the central frequency $\nu_0 = 22.235$ MHz inside the frequency interval corresponding to radial velocities $\Delta u \approx 1.02$ km s⁻¹. (The frequency shift is related to radial

velocity as $\Delta\nu = -u\nu_0/c$, where c is the velocity of light.) The superposition of these three lines represents an asymmetric total line if the Doppler widths of these lines overlap separations between them. Meanwhile, Varshalovich et al. (2006) consider only the thermal Doppler width.

The numerical calculations of the H₂O maser intensities taking the hyperfine structure of the energy level into account have been done in some papers (see, for example, Nedoluha & Watson 1986, 1991). The interesting short paper of Watson et al. (2002) is devoted to discussion when the H₂O maser line shape in saturated regime is Gaussian. In contrast to these papers, we use here the analytic expression for the H₂O maser spectral line shape derived in a recent paper by Varshalovich et al. (2006). This expression allows us to investigate the “intrinsic” mechanism of the asymmetry in detail.

The goal of our paper is to find single asymmetric spectral lines in the data of our longterm monitoring of various H₂O maser sources, analyze them and discuss whether the possible mechanism of the asymmetry is caused by the intrinsic mechanism proposed by Varshalovich et al. (2006). In addition to thermal motions of the molecules, we also take small-scale turbulent motions into account.

2. Data presentation

We use the published results of the observations on the RT-22 radio telescope RT-22 (Pushchino Radio Astronomical Observatory, Russia) of the H₂O maser emission from sources associated with active star-forming regions (see, e.g., Lekht et al. 2002, 2004). We selected lines during fairly strong bursts when the lines are not blended at a level higher than 0.05–0.07 of the

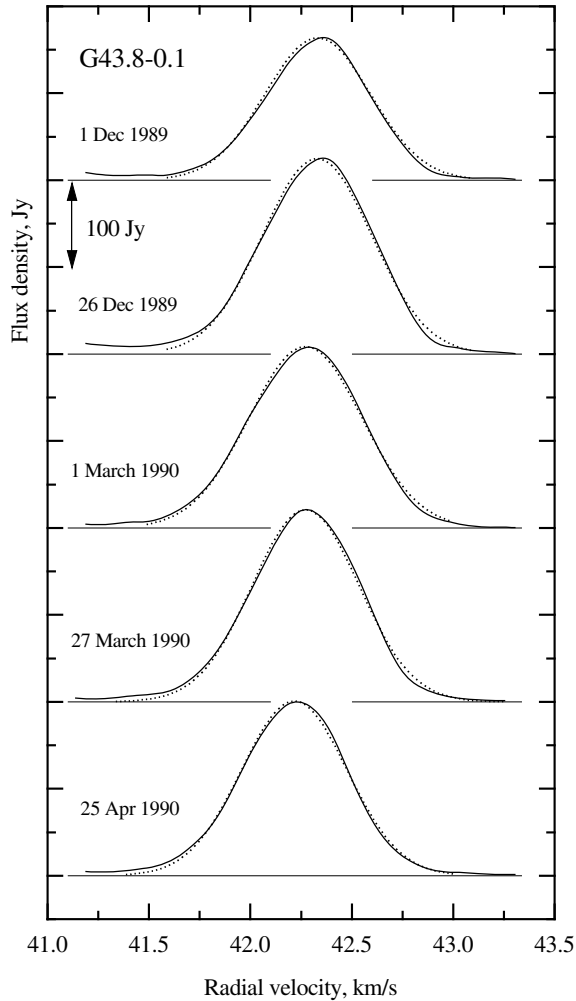


Fig. 1. a) The observed H_2O maser line in G43.8–0.1 with the non-Gaussian shape. Dotted lines represent a Gaussian fit.

peak intensity at the line center. In this case we hope that even fairly weak asymmetry can in fact be detected.

For asymmetric line profiles, we analyzed the evolution of a line; i.e., we studied the line shape throughout the active emission phase. This allowed us to exclude those cases of superposition of the emission features with closely velocities. In Fig. 1a we present the evolution for one of the flare components of the H_2O maser spectrum in G43.8–0.1 during the five months corresponding to the period of the highest flare activity. This emission feature was chosen because it has the most typical line width ($\approx 0.6 \text{ km s}^{-1}$) and because it had been observed continuously, over more than 15 years (Lekht 2000). The observed flux was much greater than the fluxes of the nearest features, the radial velocity changes during these years in a very small interval $42.2\text{--}42.4 \text{ km s}^{-1}$. The linewidth changes in the small interval $0.5\text{--}0.7 \text{ km s}^{-1}$. At an unsaturated regime, when the flux increase is accompanied by decrease in the linewidth, the line was symmetric. At the saturated regime the maser line was asymmetric, the left wing more slope than the right one. There was also the correlation between the variations in flux and the linewidth (see, e. g., Lekht 1994, 2000). Without doubt, we observed the single feature, not a superposition of features. To the left, the observation dates are given, and similar line profiles are presented for some other sources (see Figs. 1b–1c).

We have also normalized the profile amplitudes and shifted the maxima to the zero velocity. The normalized profiles are

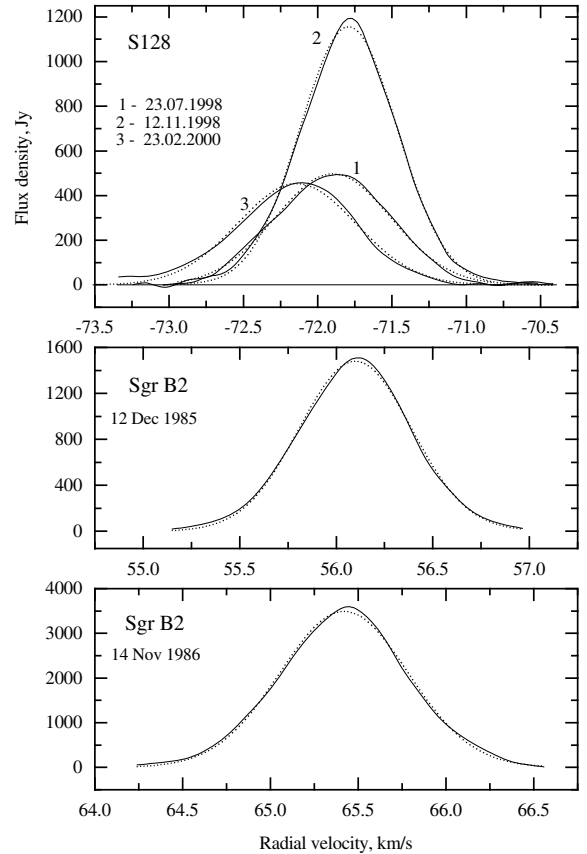


Fig. 1. b) Same as in Fig. 1a, for the sources S128 and Sgr B2.

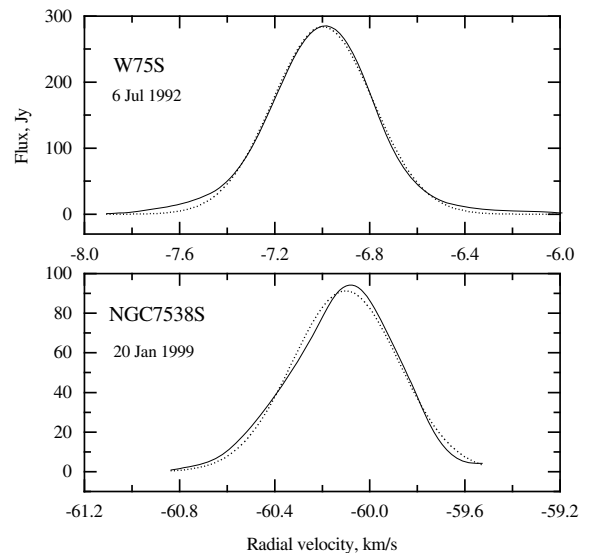


Fig. 1. c) Same as in Fig. 1a, for the sources W75S and NGC 7538S.

shown for most profiles presented in Figs. 1a–1c. They are given in Fig. 2 with bold curves. Thin lines on the profile's left sides denote the mirrored right side of the profiles to show the asymmetry. The same was done for the left-hand profiles (not presented in this paper). For the most part, such symmetrized profiles can be satisfactory approximated by Gaussian curves.

Below we discuss a possible explanation of the asymmetry by the mechanism of Varshalovich et al. (2006), starting with the possible values for the line asymmetry caused by this mechanism.

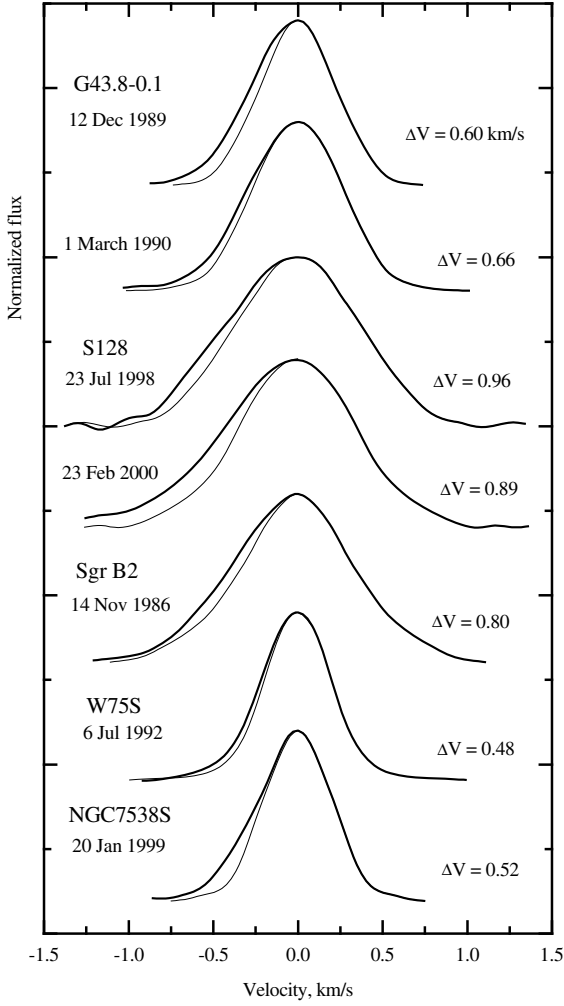


Fig. 2. Normalized line profiles of various sources of the H_2O maser emission. Thin lines represent the mirror images of the right sides of the lines. On the left the source names and observation dates are indicated. On the right we give linewidth at the 0.5 level.

3. The asymmetry due to the hyperfine structure of the H_2O maser line

According to Varshalovich et al. (2006), an asymmetric H_2O line is more intense on the left (high-frequency) side. The lines of this type most frequently show up in our observations (see Lekht 2000, 2002; and Lekht et al. 2004).

It is well known (see, Kukolich 1969; Deguchi & Watson 1986; Varshalovich et al. 2006) that the water-vapor molecule can exist in the para and ortho states. In the para state the spins of the hydrogen nuclei are antiparallel ($I = 0$), while in the ortho state they are parallel ($I = 1$). In the ortho state the hyperfine structure of the $J_{K_a K_c} = 6_{16} \rightarrow 5_{23}$ rotational transition ($\lambda = 1.35$ cm) is due to two processes: interaction of the total spin $I = 1$ with the internal magnetic field of the molecule and interaction of the proton's spins with each other.

As a result, the H_2O line at $\lambda = 1.35$ cm consists of three components corresponding to the strongest lines of the hyperfine structure. Usually, instead of frequency ν one uses corresponding radial velocities u ($\nu - \nu_0 = u \nu_0/c$) in radio astronomy. The maximum radial-velocity separation between the hyperfine triplet components is about 1.02 km s^{-1} .

Table 1. The values of radial velocities u_m corresponding to the maximum of the extinction coefficient $\phi(u)$ (see Eq. (1)), and the values of this factor at the maximum $\phi_m = \phi(u_m)$ for various effective Doppler velocities u_D .

$u_D, \text{ km s}^{-1}$	0.5	1	1.5	2	2.5	3	4
$-u_m, \text{ km s}^{-1}$	0.243	0.398	0.420	0.426	0.429	0.430	0.432
ϕ_m	0.613	0.850	0.928	0.958	0.973	0.981	0.989
$A_\phi^*, \%$	128	7.0	1.50	0.62	0.27	0.16	0.07

* Is the asymmetry of $\phi(u)$ at the profile level 0.5.

Varshalovich et al. (2006) obtained the following analytic expression for the total profile function (the extinction coefficient is proportional to this function):

$$\phi(u) = a \exp\left[-\left(\frac{u - u_a}{u_D}\right)^2\right] + b \exp\left[-\left(\frac{u - u_b}{u_D}\right)^2\right] + c \exp\left[-\left(\frac{u - u_c}{u_D}\right)^2\right], \quad (1)$$

where $a = 0.3919$, $b = 0.3302$, $c = 0.2779$ and $u_a = 0$, $u_b = -0.4458$, $u_c = -1.0293 \text{ km s}^{-1}$; here, u_D is the effective Doppler velocity. This velocity describes the Doppler width $\Delta\nu_D = \nu_0 u_D/c$, and includes contributions from the thermal velocity $u_{\text{th}}^2 = 3kT/m$ and mean small-scale turbulent velocity $u_{\text{turb}}^2 = \langle u^2(\mathbf{r}, t) \rangle$ (see, e.g., Kaplan & Pikelner 1970): $u_D^2 = 2/3(u_{\text{th}}^2 + u_{\text{turb}}^2)$. The positions of the maximum of $\phi(u)$, denoted as u_m , and the maximum values of this function $\phi_m = \phi(u_m)$ are listed in Table 1 for various values of parameter u_D . At $u_D \gg 1$ the value of $u_m \rightarrow 0.433 \text{ km s}^{-1}$.

If the effective Doppler velocity u_D is lower than the separation between the triplet components, the extinction coefficient is the sum of three separate Gaussian expressions. But if u_D is comparable to or greater than these separations ($u_D > 0.35\text{--}0.5 \text{ km s}^{-1}$), then formula (1) describes a single-peaked curve with asymmetry relative to the vertical line drawn through the curve maximum. The profile function $\phi(u)$ is skewed towards the blue (negative radial velocities). For convenience, we shifted the maximum position u_m to the point $u = 0$.

To describe the asymmetry of the line profile, we introduce the degree of asymmetry (see also Silant'ev et al. 2002):

$$A_\phi(u) = \frac{\phi_L(u) - \phi_R(u)}{\phi_{\text{mean}}(u)} = \frac{\phi(-u) - \phi(u)}{(\phi(-u) + \phi(u))/2}, \quad (2)$$

where $u = 0$ henceforth corresponds to the maximum of the profile function $\phi(u)$; $u < 0$ corresponds to the left side (high frequency) of the profile, and $u > 0$ to the right side. Remember that Varshalovich et al. (2006) introduced a different definition of the asymmetry coefficient

$$\xi_\phi(u) = \phi_L(u)/\phi_R(u). \quad (3)$$

These parameters are related by the formula

$$\xi_\phi(u) = \frac{2 - A_\phi(u)}{2 + A_\phi(u)} > 0. \quad (4)$$

According to Eq. (1), the blue side of the profile is higher than the red one. Ultimately, $A_\phi \rightarrow \pm 2$ at $u \gg 1$ depending on the inequalities $u_L > u_R$ or $u_L < u_R$. The values of A_ϕ at the profile half-maximum level are listed in Table 1. We see that the degree of asymmetry A_ϕ quickly tends to zero with the increase in the effective Doppler velocity u_D .

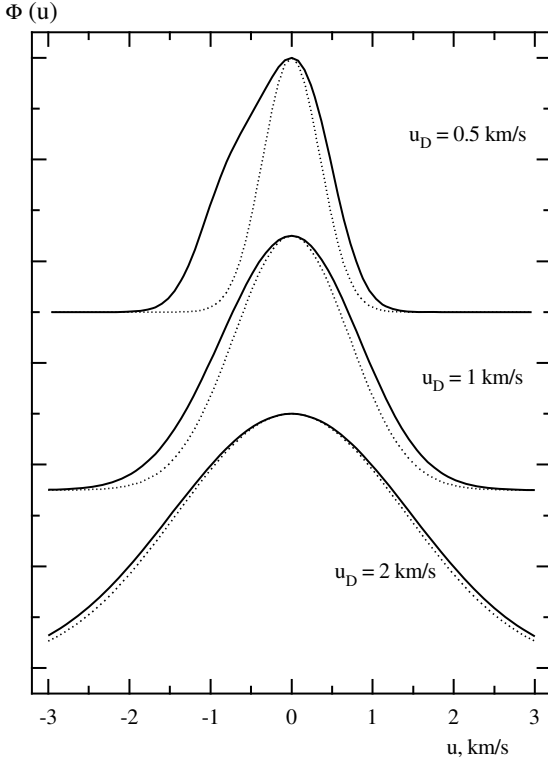


Fig. 3. The comparison of the normalized profiles $\Phi(u)$ with the Gaussian profiles $\Phi_0(u) = \exp[-(u/u_D)^2]$ (dotted lines) for various values of the effective Doppler velocity u_D .

At $u_D < 0.5\text{--}1 \text{ km s}^{-1}$, the shape of the extinction coefficient differs strongly from the Gaussian form. To consider this difference in more detail, we introduce the normalized extinction factor

$$\Phi(u) = \phi(u)/\phi_m, \quad (5)$$

i.e., $\Phi = 1$ at $u = 0$. Sometimes it is convenient to use the dimensionless frequency $x = (v-v_0)/\Delta\nu_D = u/u_D$ and to compare $\Phi(x)$ with the usual normalized profile function $\exp(-x^2) \equiv \Phi_0(x)$.

The comparison of $\Phi(u)$ with $\Phi_0(u)$ (see Fig. 3) shows that the normalized profile function $\Phi(u) \rightarrow \Phi_0(u)$ with the increase in the effective Doppler velocity u_D . Simultaneously the degree of asymmetry tends to zero. The inequality $\Phi(u) \geq \Phi_0(u)$ takes place at all values of u . This inequality becomes stronger with the recession from the line center. Figure 3 also shows that for $u_D \geq 2 \text{ km s}^{-1}$ the contribution of all three hyperfine structure lines is virtually equivalent to the usual Gaussian profile function of the H_2O maser spectral line.

3.1. The line asymmetry by the radiation propagation at the unsaturated regime

At the unsaturated regime, the propagation of radiation in a medium with inverted population of energy levels the intensity is described by the formula

$$I(u) = I_0 e^{\tau\Phi(u)}, \quad (6)$$

where $\tau > 0$ is the magnitude of optical depth at the line center. Remember that $u = 0$ ($x = 0$) corresponds to the value u_m when the extinction coefficient $\phi(u)$ acquires the maximum value ϕ_m (see Table 1). The value of I_0 denotes some initial intensity (the

“seed” intensity) at the beginning of the maser line formation process.

The asymmetry in $\Phi(u)$ obviously gives rise to asymmetry in intensity $I(u)$. To study the line shape we introduce normalized intensity (below we use the dimensionless frequency x)

$$J(x) = \frac{I(x)}{I_{\max}} \equiv e^{\tau(\Phi(x)-1)}. \quad (7)$$

Since $\Phi(0) = 1$, we set $J(0) = 1$.

Usually one uses the normalized intensity

$$J_0(x) = e^{\tau(e^{-x^2}-1)}, \quad (8)$$

which corresponds to symmetric Gaussian profile function $\Phi_0(x) = \exp(-x^2)$.

Normalized intensity with the Gaussian form $\Phi_0(x)$ at large τ virtually coincides with the expression $J(x) = \exp(-\tau x^2)$, i.e., as first mentioned by Strelnitsky (1982), has a Gaussian shape. Below we present the analytic proof of this general statement.

For low values $x = u/u_D \ll 1$, this is evident from the power-law expansion of the exponent function $\exp(-x^2) \approx 1 - x^2 + \dots$

$$J_0(x) = e^{\tau(e^{-x^2}-1)} \approx e^{-\tau x^2}. \quad (9)$$

Let us denote as J_1 the value of $J_0(x)$ at arbitrary value x_1 . The value J_1 occurs at

$$x_1^2 = -\ln\left(1 + \frac{\ln(J_1)}{\tau}\right) \rightarrow \frac{|\ln(J_1)|}{\tau}, \quad \tau \gg 1. \quad (10)$$

For Gaussian curve $\exp(-\tau x_1^2)$, the value J_1 takes place at

$$x_1^2 = \frac{|\ln(J_1)|}{\tau}. \quad (11)$$

Both expressions (10) and (11) coincide with one another for large τ , when the inequality $|\ln(J_1)|/\tau \ll 1$ holds. Thus, in the middle of a profile ($J_1 = 0.5$) the x_1 -values are equal to 0.2680 and 0.2632 at $\tau = 10$ according to formulas for $J_0(x)$ and $\exp(-\tau x^2)$, respectively.

From Eqs. (10) and (11), it follows that the linewidth for $\tau \gg 1$ is proportional to $1/\sqrt{\tau}$ (see Goldreich & Kwan 1974; and Strelnitskij 1982). Below we shall see that this also approximately exists for normalized maser intensity (7), which does not have a Gaussian shape. For high effective Doppler velocity $u_D > 1\text{--}2$, the extinction coefficient $\Phi(u) \rightarrow \exp(-u^2/u_D^2)$, and the line shape also acquires the Gaussian form at large τ .

The degree of the line asymmetry is defined analogously to expression (2) for $A_\phi(u)$:

$$A_J(u) = 2 \frac{e^{\tau(\Phi(-u)-\Phi(u))} - 1}{e^{\tau(\Phi(-u)-\Phi(u))} + 1} \equiv 2 \tanh(2\tau[\Phi(-u) - \Phi(u)]). \quad (12)$$

For high values of τ , formula (12) yields the maximum value $A_J = \pm 2$, depending on whether I_L or I_R is greater.

In Table 2 we list the values of A_J and the linewidths at the profile half-maximum for various values of τ and effective Doppler velocities u_D . It is visible that the linewidths decrease approximately as $1/\sqrt{\tau}$. This means that the velocities u , corresponding to this level, also decrease. For this reason the A_J coefficient at the level $J = 0.5$ decreases with the increase in optical lengths τ because the asymmetry of the extinction factor near the line center tends to zero. Of course, for the fixed value of the velocity u , the increase in τ gives rise to an increase in

Table 2. The linewidths $(\Delta u)_{0.5}$, and the asymmetry degree $(A_J)_{0.5}$ of the unsaturated maser line after the propagation of optical length τ (in the center of a line) taken at the profile level 0.5.

τ	$(\Delta u)_{0.5}$, km s ⁻¹			$(A_J)_{0.5}$, %		
	$u_D = 0.5$	1	2 km s ⁻¹	$u_D = 0.5$	1	2 km s ⁻¹
10	0.44	0.64	1.12	27	2.65	0.27
15	0.34	0.52	0.91	21	2.20	0.26
20	0.29	0.45	0.79	18	1.95	0.26
25	0.26	0.40	0.70	15	1.80	0.26
30	0.24	0.36	0.64	14	1.70	0.26
35	0.22	0.34	0.59	13	1.60	0.26
40	0.20	0.32	0.55	11	1.50	0.26

the asymmetry, so for the case of $u_D = 1$ km s⁻¹ at fixed value $x = 0.5$, where $A_\phi = 1\%$, we have the degrees of asymmetry $A_J = 10.5\%$, 16.5% , and 24.7% for $\tau = 10, 20$, and 30 , respectively. Evidently, the exponential, i.e. nonlinear, increase in intensity (6) also increases the asymmetry of a maser line very strongly.

3.2. The line asymmetry at saturate regime of the radiation propagation

In the saturated regime, the radiation intensity $I(x, \tau)$ obeys the nonlinear transfer equation (see, for example, Litvak 1970; Goldreich & Kwan 1974; Elitzur 1992; and Watson et al. 2002) of the form

$$\frac{dI(x, \tau)}{d\tau} = \frac{\Phi(x)I(x, \tau)}{1 + b(x)I(x, \tau)}, \quad (13)$$

where the term bI describes the decrease in the number of inverted molecules due to stimulated emission. (It depends on Einstein coefficient B_{21} and beaming angle $\Delta\Omega$ of maser radiation.) For detailed explanations we refer to the cited references. If $bI \ll 1$, we return to the unsaturated regime. For $bI \gg 1$, we are in a linear amplification regime, where $I \propto \tau\Phi(x)$. The formal solution of Eq. (13) has the form (see Watson et al. 2002):

$$I(x, \tau) = I_0 e^{-b(x)I(x, \tau)} e^{\tau\Phi(x)}. \quad (14)$$

The saturated regime is initiated at the center of a line ($x = 0$) where the intensity is greatest. For other frequencies, this regime begins at larger τ . Watson et al. (2002) used Eq. (14) with the Gaussian profile $\Phi(x) = \Phi_0(x) = \exp(-x^2)$ of the extinction coefficient to investigate numerically when the line shape is near the Gaussian form. In their case, the profile of maser line is symmetric ab initio. They found that the line shape is near Gaussian one if the pumping region has a very high temperature of $900 < T < 3000$ K. This result seems natural for such wide linewidths of the extinction coefficient. The analytic investigation, like our approach in the previous subsection, for nonlinear expression (14) does not exist.

We investigated the asymmetry $A_J(x, \tau)$ of the maser line in the saturated regime using the nonlinear solution (14) with asymmetric profile $\Phi(x)$. The problem depends on parameters u_D, τ and b . Besides, due to a nonlinearity of expression (14) there exists the dependence on the value of initial intensity I_0 . The main result is that the degree of asymmetry in saturated regime is greater (in many cases much greater) than in unsaturated one.

The main reason for the increase in asymmetry is that, in wings of the maser line, the saturated regime occurs at greater optical depth τ than in the center of a line. When in the center ($x = 0$) the radiation increases linearly $\sim \tau\Phi(x)$, in the wings the radiation continues increase exponentially $\sim \exp(\tau\Phi(x))$. Besides, remember that the asymmetry of the profile $\Phi(x)$ is greater in the wings than near the center. This gives rise to large increase in asymmetry in saturated regime. The same reason gives rise to the line rebroadening (see Goldreich & Kwan 1974).

The nonlinearity of the saturation process gives rise to the decrease in final asymmetry with the decrease in the ‘‘seed’’ intensity I_0 . The decrease of I_0 moves the region of τ when saturation regime occurs to the outer boundary of the layer of pumping region. As a result, the region of saturation regime diminishes, and the asymmetry lessens. Thus, for $\tau = 10, b = 0.001$, and $I_0 = 1, 0.1$, we obtained the value 77% in first case for A_J at the middle of a line ($J = 0.5$), and 46% in the second one. The linewidths in these cases are 0.75 and 0.56 km s⁻¹, respectively. In the unsaturated regime, the asymmetry is 28% and the linewidth 0.42 km s⁻¹. In these cases we take $u_D = 0.5$ km s⁻¹. These calculations show that the linewidth in the saturated regime is greater than in the unsaturated one (the line rebroaden effect). Note that if $u_D = 1$ km s⁻¹ the corresponding degrees of asymmetry are $A_J = 5\%$, 3.7% , and 2.65% .

As a result, the saturation regime can produce fairly large asymmetry as compared with the unsaturated one, especially for $u_D \sim 0.5$. Because of very complex dependence of the asymmetry on all the parameters, we restricted ourselves to these model examples and their qualitative explanation.

4. Data analysis and discussion

We first discuss the explanation of the observed asymmetry in the model unsaturated maser propagation. The results presented in Fig. 2 demonstrate that the degree of asymmetry A_J at the level $J = 0.5$ can be fairly high, ≈ 10 – 40% . In this case, the linewidths Δu are also large, ≈ 0.5 – 1 km s⁻¹. The estimations of optical lengths τ yield $\tau \approx 30$ – 35 (see Strelnitskij 1982). Taking into account that the observed lines narrow its widths during the propagation as $1/\sqrt{\tau}$, we conclude that the effective Doppler velocities have to be $u_D > 2$ km s⁻¹.

Such high Doppler velocities cannot be accounted for by thermal velocities. Indeed, maximum temperatures for which the inverted medium for H₂O molecules can exist are 600–1000 K (see Varshalovich et al. 2006). These temperatures correspond to the effective Doppler velocities ≈ 0.75 – 0.95 km s⁻¹. This is far from the mentioned lower limit of 2 km s⁻¹. The minimum required small-scale turbulent velocities are $u_{\text{turb}} \approx 2.1$ – 2.3 km s⁻¹.

Table 2 demonstrates that, for the effective Doppler velocities $u_D > 2$ km s⁻¹, the asymmetry of the lines is very low, less than 0.25% . Such a low value is the consequence of the fact that the shape of the extinction coefficient virtually coincides with a symmetric Gaussian curve for these values of u_D . (From Table 1 it is visible that asymmetry A_ϕ at the level $\Phi = 0.5$ is less than 0.6% .) This means that the observed asymmetry of the maser lines presented in Fig. 2 cannot be explained directly by the mechanism of Varshalovich et al. (2006). Nevertheless, this mechanism can explain the line asymmetry in very narrow maser lines, with widths $\Delta u \approx 0.2$ – 0.4 km s⁻¹, which correspond to effective Doppler velocities $u_D \leq 0.5$ (temperature $T \leq 600$ K). Table 2 describes the results for an unsaturated maser.

Let us consider now the application of the mechanism of Varshalovich et al. to saturated masers. According to

Lekht (2000), the maser emission at 42.2 km s^{-1} in G43.8–0.1 was observed in various states of the maser saturation. The spectra presented in Fig. 1a refer to the period when the maser was saturated or near this state. During this time the line shape was asymmetric. During the periods corresponding to the unsaturated regime (decreasing linewidth with increasing flux), the line was symmetric. Another emission feature in this source at 38.2 km s^{-1} was also observed during its strong burst as a symmetric line with a decrease in the linewidth corresponding to an increase in the flux density. Thus, we see that the observed line is asymmetric when the maser is near the saturated regime.

In the saturated regime, the rebroadening of the maser line occurs, and the line can acquire the width equal to the width of the extinction profile $\Phi(u)$ (see Goldreich & Kwan 1974). In this case the proportionality $\Delta u \propto 1/\sqrt{\tau}$ does not take place, and we are not restricted by the condition that the width of profile function has to be more than the observed linewidth. This case can occur when these widths have the same order of magnitude, in particular, corresponding to $u_D \approx 0.5 \text{ km s}^{-1}$. We know that the case $u_D \approx 0.5 \text{ km s}^{-1}$ corresponds to high values of the profile asymmetry. Our high values of the line asymmetry $\approx 40\%$ can easily be explained in this case. Moreover, that the masers with fairly high asymmetry occurs rarely can be explained that such coincidences of widths are rare, indeed.

The asymmetry increases if in the inverted medium there exists a small radial-velocity gradient. Calculations show that this additional increase is not large: say, instead of 27%, we can obtain 30%. A large gradient destroys the maser line shape and does not allow us to obtain a large amplification of the emission.

Finally, we treat another explanation of the line asymmetry by a non-intrinsic mechanism as proposed and discussed in detail by Silant'ev et al. (2002) (see also the Introduction). According to this simple mechanism, an asymmetry degree of 10–40% can be explained by the existence of a layer of non-inverted molecules with an optical depth at the line center on the order of 2–5. There exists a relative line-of-sight velocity between the layer and the maser “spot”. The main problem in this explanation is whether such a moving layer of non-inverted molecules exists or not.

For unsaturated masers, right-hand asymmetry can only be produced by the non-intrinsic mechanism. But the left-hand asymmetry can be produced by both mechanisms, and we can hardly distinguish between them in this case.

5. Summary

We have reported the main results of the analysis of the H₂O maser line asymmetry. We have studied in detail the known

mechanism of the origin of the line shape asymmetry due to the existence of the hyperfine structure of the $6_{16} \rightarrow 5_{23}$ transition and to different (not equidistant) positions of the corresponding triplet components.

1. The triplet of the lines is characterized by the sum of the extinction factors that are continuously transformed to a single-peaked asymmetric extinction coefficient with the increase in the effective Doppler velocity u_D .
2. The noticeable asymmetry in an unsaturated maser line can only arise at $u_D \leq 0.5 \text{ km s}^{-1}$ for masers with very small linewidths $\approx 0.2\text{--}0.4 \text{ km s}^{-1}$.
3. We found that our observed unsaturated maser lines have no asymmetry, and saturated ones possess a fairly high degree of the line asymmetry, 10–40%.
4. Most probably the large asymmetry of saturated masers occurs when the rebroadening of the linewidth give rise to the value comparable to the width of profile function with $u_D \approx 0.5 \text{ km s}^{-1}$. This explains why the masers with large asymmetry are rare.

Acknowledgements. This work was supported by the Russian Foundation for Basic Research (project code 06-02-16806-a). The 22-m radio telescope is supported by the Ministry of Industry and Science of the Russian Federation (facility registration number 01-10). The authors thank the staff of the Pushchino Radio Astronomy Observatory for their extensive help with the observations. The authors are very grateful to an anonymous referee and Dr. Walmsley for numerous remarks that allowed us to clarify the paper.

References

- Deguchi, S., & Watson, W. D. 1986, *ApJ*, 302, 750
 Elitzur, M. 1992, *Astronomical masers* (Dordrecht: Kluwer Acad. Publ.), 117
 Goldreich, P., & Kwan, J. 1974, *ApJ*, 190, 27
 Kaplan, S. A., & Pikelner, S. B. 1970, *The interstellar medium*, (Cambridge, Massachusetts: Harvard University Press)
 Kukolich, S. 1969, *J. Chem. Phys.*, 50, 3751
 Lekht, E. E. 1994, *Astr. Rep.*, 31, 49
 Lekht, E. E. 2000, *A&ASS*, 141, 185
 Lekht, E. E. 2002, *Astr. Rep.*, 46, 57
 Lekht, E. E., Ramírez-Hernández, O., Tolmachev, A. M., & Berulis, I. I. 2004, *Astr. Rep.*, 48, 171
 Litvak, M. M. 1970, *Phys. Rev. A*, 2, 2107
 Nedoluha, G. E., & Watson, W. D. 1991, *ApJ*, 367, L63
 Silant'ev, N. A., Lekht, E. E., Mendoza-Torres, J. E., & Tolmachev, A. M. 2002, *Astr. Lett.*, 28, 217
 Strel'nitskij, V. S. 1982, *SvAL*, 8, 86
 Varshalovich, D. A., Ivanchik, A. V., & Babkovskaya, N. S. 2006, *Astr. Lett.*, 32, 29
 Watson, W. D., Sarma, A. P., & Singleton, M. S. 2002, *ApJ*, 570, L37